Suggestions for Tele-Seismic Hypocentre Location using Table-driven Scanning

George R. Daglish, *Member*, *IAENG*, Yuri P. Sizov, *Member*, *EAGS*

Abstract – **This paper attempts to describe a small subsystem, intended to form part of a body of intelligenced Seismic software, which is primarily:**

1. **To perform rapid determination of Hypocentres, once appropriate Epicentres are known**
2. **To form a Simulation System to assess such a process**
3. **To test models of EarthVelocity Structure (e.g. PREM, iasp91, ak135), as well as the efficacy of various point-to-point Ray Tracing techniques**

In effect, this system is a table-driven scan and works on tabular data-structures set up by combining an appropriate point-to-point Ray Tracer with any particular Velocity Structure proposed for Earth Interior.

Index Terms – **Seismics, Hypocentre, Scan, Ray-trace, Table-driven.**

I INTRODUCTION

In a previous paper involving the present authors, [1], it had been noted that there have been recent and severe disasters involving coupling between Earthquake fault-slips and the generation of Tsunami.

In response to this it is sought to automate the process of solving an Inverse Problem, in this case the determination of Event Epicentre coordinates from Energy-onset Timings, in a reliable and rapid manner.

Suggestions for this have already been laid out in [1] and the present report describes how this system may lead onto, and trigger, a very rapid Hypocentre determination with Take-off angle identification.

This determination is in the form of a Table-driven scan supported by point-to-point Ray Tracing and Linear, Cubic or Lagrange interpolation.

Manuscript received March 29, 2012; revised April 10, 2012.
G. R. Daglish is a Consultant with Independent Analysis and Computation at 9 Partridge Close, Frimley CAMBERLEY, Surrey. GU16 8PD. UK. +44 (0)1276 26942.George.daglish@tiscali.co.uk. Yu. P. Sizov is with the GeoElectroMagnetic Research Institiute, (where he is Scientific Secretary), at GEMRI. PO BOX 30. 142190 Troitsk, Moscow Region. RUSSIA. Sizovyur1@yandex.ru

II THE STATIC STRUCTURE

Two versions of this structure exist. They are each based on the properties of the point-to point Ray Tracing algorithms which are used to generate the Tables which are to drive this Hypocentral Scan. The general form for both these structures is depicted at **Figure 10.**

The prime Data Table consists, in each case, of a set of vectors whose elements are timing values (ray travel times). Each vector corresponds to a point of Relative Latitude [Latitudinal Distance]. The set of timing values within each of them correspond to a constant set of Depths. In this case, a uniform Earth radius is taken to be 6367.65 km. I.e. this table system is a set of scalar fields whose independent axes are Relative Latitude and Depth, with field values for take-off angles; accuracy measures [weightings] and the above mentioned timings.

This displacement [or Relative Latitude] is considered relative to the Event epicentre, whose latitude is taken as Zero reference. We can distinguish between the cases where the vector of displacements is chosen as an abstract or general grid, and where this vector is based upon known and selected Stations.

Evidently, a general set of tables runs a risk of introducing higher error than one based on known relative Latitudinal Distances, for a set of previously determined Stations. However, if the tables are built around such previously selected Stations, then this process of table-building can only start **after** the Epicentre for the incoming Event has been determined. Table-building is a costly process in time. This would, therefore, degrade the system response. The first method, using general pre-constructed tables can find Hypocentre Foci within times of **order** $<$ **0.25 second** [Dell XPS600 at 3.2 GigaHertz under Microsoft™ Windows XP™]. So that, from the point in time of knowing the Event Epicentre, the Hypocentre and Take-off angles can be made available within 0.25 seconds of processing time. Means therefore should be found to minimise the error-inducing self-noise inherent in general tables.

An example of such a structure is given at **Figure 1**.

Self-noise within this sub-system as a whole (the "whole" comprising: generation of Data Tables **and** Location of

ISBN: 978-988-19252-1-3
ISSN: 2078-0958 (Print); ISSN: 2078-0966 (Online)

Hypocentre by scanning Data Tables) arises from several prime causes:

1. Inaccuracy in the trajectory (and thus the Travel Times), of the rays generated by the point-to-point Ray Tracers
2. Error by the Interpolation routines in looking up Travel Times from these tables
3. Granularity of the scanning interval chosen

Additionally to this self-noise, noise would also appear to arise from the following sources:

1. Adequacy of the radial Earth Velocity Model used
2. Variation of Earth from perfect sphere
3. Variation of Earth radii subtended at Stations
4. Accuracy in recording the onset times of the P-, S-, L- and R-wave species.

The two versions of this proposed structure correspond to two distinct types of point-to-point Ray Tracing algorithms based on:

1. a Lagrangian Formulation and Approach [LFA] for the control of its convergence [2] [3][4].
2. a development of the Ray Equation [5]:

$$\nabla u - \frac{\partial}{\partial s}\left(\left(\frac{1}{v}\right)\cdot\frac{\partial \underline{r}}{\partial s}\right) = Zero;$$
$$\left(u = \frac{1}{v(x,y,z)}\right);\ \underline{r} = (x,y,z).$$

Both use a radial Earth Velocity model within spherical and concentric layers of velocity variation. Such a model is depicted at **Figure 2**. u, above, is the "slowness" and v is the velocity, both as 3-space scalar fields.

In the original system diagram, program modules are bracketed in **BLACK,** while files of data, holding tables, are bracketed in **RED**. The entity identification is found within the brackets. Data flow is shown as **BLUE** arrows and input of a single parameter is indicated as a symbol accompanied by an arrow in **RED**.

With regard to the **first point-to-point algorithm**, [2] [3] [4],the symbol ψ_0 represents a set of take-off angles. Initially a suitable take-off angle is introduced as a single parameter. The process "11", is able to accept a table of take-offs $[\psi_0]$ or a single parametric value, ψ_0. Using this input it produces a table of take-off angles together with a table of Travel times, $[T]$. These times represent arrivals at a given set of equally spaced Latitudinal Distances from the Epicentre, considered as pole, and ranging currently from one to ninety degrees. In this we are ignoring shadow zones and the small region between ca. 165 degrees and 180 degrees to which rays may pass.

As output, the process "11" produces an intermediate set of tables, $[C00]$ and $[C01]$. These contain an initially output set of take-off angles and a set of travel times (together with vectors $[V]$, containing values for the axial quantities framing the tables, namely radial depth within the Earth, H_d, and the graduated set of Latitudinal Distances).

The content of the entity $[C00]$ is moved to the first version of the $[\psi_0]$ table. (This table can be used as input for subsequent cycles of the setup procedure devolving around process "11" to refine the values in $[\psi_0]$).

The file $[C01]$ splits up into the vectors containing the axial quantities, $[V]$, and into the corresponding table of Travel or Arrival timings, $[T]$. These three files are input to either one of the processes: "9", "12" or "13" which will use them parametrically to perform a scan to realize the Hypocentral Depth, H_d

In the case of the **second point-to-point algorithm** [5] the process is similar but does not include a priming version for the take-off angle, which is not needed in this case, since the steering loop scans for a hit on the target point using a "binary chop" procedure. The resulting values found for ψ_0 are placed likewise in $[C00]$, but no further refinement is necessary.

III THE SCANNING PROCESS

This has initially been described at SECTION VI in [1]. The processes "9", "12" and "13", given at **Figure 10**, contain a routine which can interpolate in a linear or non-linear manner. These routines scan radially upward in depth and, by interpolation from the tables given above, calculate:

- A vector of travel times to the chosen set of Stations from each depth point on the radius subtended by the Epicentre.
- A corresponding vector of take-off angles leading to each Station.

For each depth point around which data has been constructed in $[V]$ and $[T]$ above, the extracted vector of travel times is centralized around its mean as a set of residuals. This set of residuals is compared with the set of residuals formed in a similar manner from the arrival times, at the chosen Stations,

ISBN: 978-988-19252-1-3
ISSN: 2078-0958 (Print); ISSN: 2078-0966 (Online)

of the rays emanating from the object Event. This procedure is described at the final section of [1]. The difference is measured as an RMS minimum, where the RMS of the differences between the residuals at each depth is used to locate a probable value for the Hypocentral Depth, H_d.

The overall scanning process, given at **Figure 10**, and scanning upwards or downwards as above, can currently compare four 2-space interpolation schemes in parallel:

1. Depth: Linear; Latitude: Linear
2. Depth: Cubic; Latitude: Linear
3. Depth: Cubic; Latitude: Cubic
4. Depth: Lagrange; Latitude: Lagrange

The **Figures 3, 4 & 5, 6**, are each the results of a 533 point scan along a radial path, from a depth of 1000 km, to the Earth surface. The reason for the odd granularity of scan is to exercise the Interpolation Regime chosen, since the data tables, themselves, are formed from 100 × 101 element matrices: 100 for depths and 101 for the Latitudinal Displacements. In the group of tables generated for this set of tests the depths spanned 10 to 1000 km in steps of 10 km.

All Self-tests have Station Latitudes non-aligned with the Latitudinal Displacements chosen to form the tables. This will exercise the Latitudinal part of the interpolation regimes.

The discrepancy in these cases is calculated as:

$$|\Delta\lambda| * R_e$$

where $\Delta\lambda$ is the difference in angle between the required Latitude and that realized by the Ray Trace. R_e is an appropriate Earth Radius. This discrepancy value currently resides in the interval:

$$[1.0_{10}-10,\ 1.0_{10}-5].$$

So here the self-noise is low.

Some unsuccessful Self-tests are exemplified by **Figures 7** and **8**, and an example of the output of the second Ray Tracer is given at **Figure 9**.

IV DISCUSSION

To recapitulate the initial statement concerning the times at which the Data Structures should be determined, we may say: if the Data Structure is determined prior to the Event then several variants can economically be tried out on the incoming P-wave arrivals – since individual scans may take place in a time interval **less than 0.25s** [Dell XPS600; 3.2 GHz; Microsoft ™ Windows XP ™]. This would be the prime strategy.

A second strategy is to generate the structures **using those Stations in receipt of P-waves** from the Event, once the Epicentre has been determined. To save time High Performance computing would be needed, since 10,100 ray traces would be required. However, each trace is independent so this generation of data for scanning may offer a high degree of parallelism.

The third strategy is simply to scan in Depth, once the Epicentre of the Event has been determined. This also introduces opportunity for parallelism.

The first strategy suffers from self-noise originating from three sources:

- Ray Trace point-to-point accuracy.
- Interpolation in Latitudinal Distances
- Interpolation in Depth.

The second strategy self-noise arises from two sources:

- Ray Trace point-to-point accuracy.
- Interpolation in Depth.

The third strategy suffers only from self-noise due to the point-to-point accuracy of the Ray Tracer(s) employed.

The discussion in this report is limited to the magnitude of the self-noise to be found in the two versions of the Ray Tracing systems.

It was noted at section II that the process, **dependent on the first form of ray tracer**, can be initiated by a single parametric value for ψ_0 which then generates the first version of the table $[\psi_0]$. Owing to the nature of the currently chosen ray tracer which uses two interlocking feed-back loops, [2], [3], [4], it is possible to refine this first version of $[\psi_0]$ by re-inputting it to the setup procedure that revolves around the process "11". This will result in an improvement in those areas of the subsystem which are affected by currently incomplete convergence onto true (or truer) take-off angles.

While the tables $[\psi_0]$, $[V]$ and $[T]$ take some time to prepare, the time needed for a Scan looking up these tables with interpolation is startlingly short.

Preparing the two tables, $[\psi_0]$ and $[T]$ each of size 100×101 elements, (Depths by Latitudinal Distances), takes up to four/five hours, when attempting to maximize convergence on the required values. However, performing a 1000-step scan in quadruple precision, using, say, a set of seven widely spaced Stations (from 5^0 to 80^0 of arc), takes place **within 0.25 second** on a Dell XPS600 with a frequency of 3.2 GHz under M/S Windows XP ™ operating system.

ISBN: 978-988-19252-1-3
ISSN: 2078-0958 (Print); ISSN: 2078-0966 (Online)

This leads to the possibility of having a set of tables constructed from several combinations of Earth Models and Ray tracers and assessing the relative suitability of each combination, and/or running them in parallel under active usage.

Such a parallel comparison is, in fact, performed by the system **based on the second form of ray tracer** given in this report. In this, as mentioned at Section III, the four interpolation regimes are run and compared in parallel.

Accompanying such graphs may be their Accumulating Mean Error calculated at each given Hypocentral depth:

$$\overline{e}_i = \frac{1}{i} \cdot \left(\overline{e}_{i-1} \cdot (i-1) + |e_i| \right)$$

or a graph of the pointwise individual error made with each located Hypocentre.

This first set of trials exercises the first Ray Tracer, formed from Lagrangian controlling loops [2] [3] [4]. The second set of trials involves the second algorithm, formed directly from the Ray Equation [5]. Results of this are shown at **Figures 3, 4** givng results from the use of the first Ray Tracer and **Figures 5, 6** giving results from the second**..**

On scrutiny one observes several features that the two sets of trials possess in common:

1. Soon after or at about a depth of 700 km there is a step in the level of self-noise.
2. At or about a depth of 240 km there is a large spike in the error associated with the Hypocentral location
3. At or around 50 km there also appear to be difficulties in both the locating processes.

These features would appear to correspond to the following aspects of the Earth Velocity Model employed here:

1. A jump discontinuity in the velocity model – the velocity moving from ca 10.6 to 10.0 km/s at 700 km.
2. At 250 km there is a sharp inversion in the velocity gradient, moving from decreasing to increasing at this point. This implies a jump discontinuity in the first derivative.
3. At ca 50 km there is a second sharp inversion in gradient, from increasing to decreasing.

In these regions, the self-error seems well contained by the **second form** of the Ray Trace and Scanning Algorithms. However, the **first form**, based on the Lagrangian Formulation and Approach for its method of control, would yet appear to need more refinement.

REFERENCES

[1] “Suggestions for the Structure of Kernel Software in Intelligent Seismic Nets”. Daglish GR , Sizov YuP, World Congress on Engineering, London. 2011.

[2] “Lagrangian Point-to-Point Ray Trace within Earth co-Spherical Layers to perform Hypocentral Scan”. Daglish GR. [unpublished paper]. 2011.

[3] “A Perturbation Method, which achieves accurate Point-to-Point Ray Traces, and its Context”. Daglish GR, ICSPTA 2010, Jiao Tong University, Shanghai, PR China, 2010.

[4] “Advances in Seismic Event Location”. Thurber CH, Rabinovitz N, Kluwer, 2000.

[5] “Principles and Applications of Microearthquake Networks”. Lee WHK, Stewart SW. Academic Press. 1981.

ISBN: 978-988-19252-1-3
ISSN: 2078-0958 (Print); ISSN: 2078-0966 (Online)

.

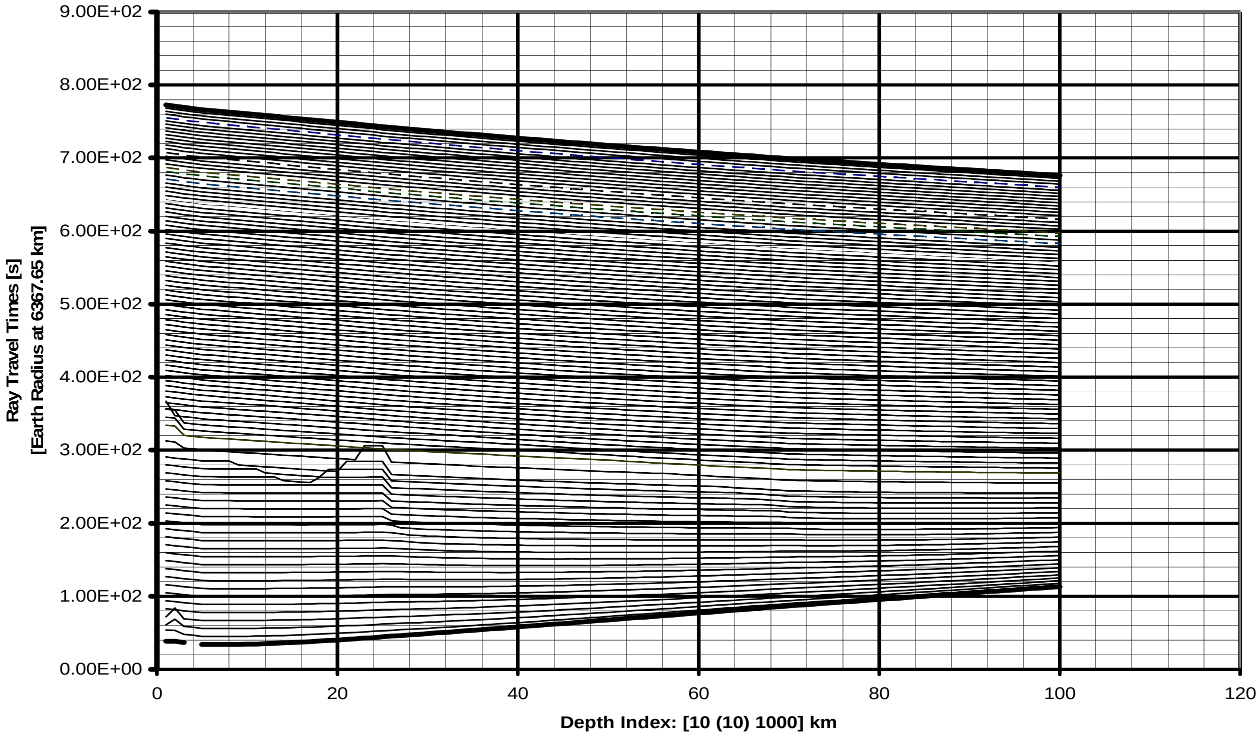

Figure 1. Scanning Data Structure [Timing (s) vs. Depth Index]

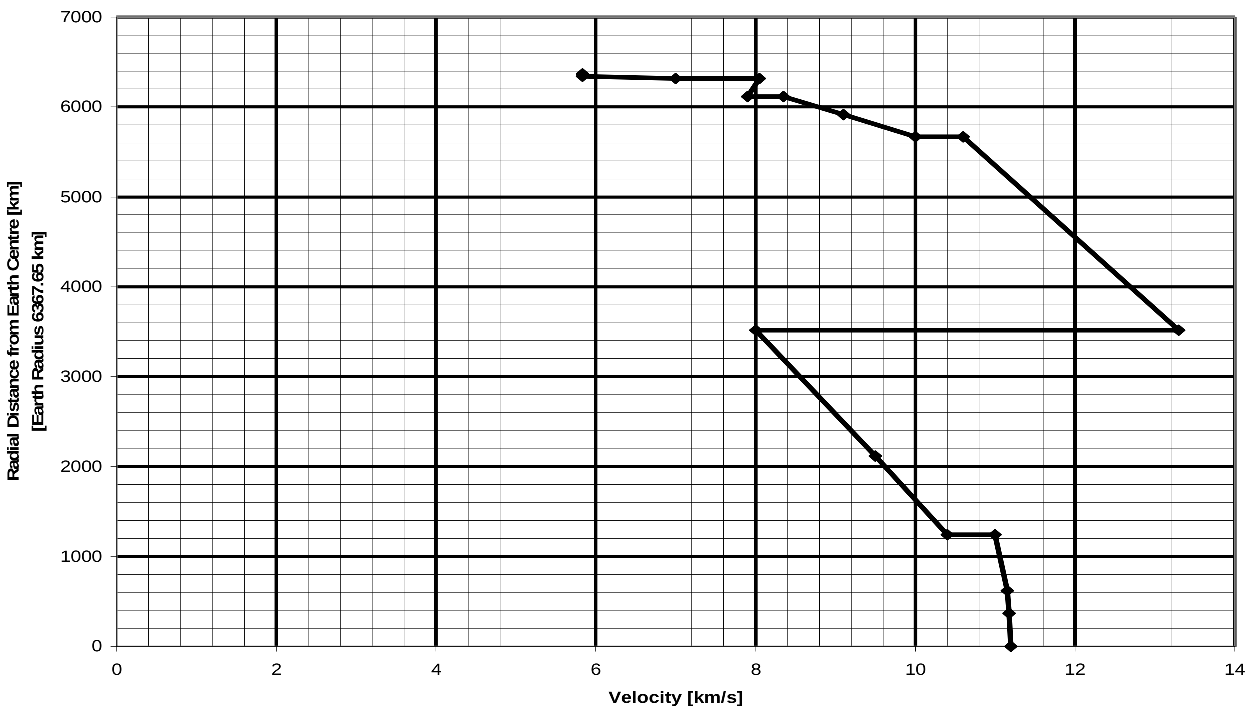

Figure 2. Velocity Profile [Earth Radius (km) vs. Velocity]

ISBN: 978-988-19252-1-3
ISSN: 2078-0958 (Print); ISSN: 2078-0966 (Online)

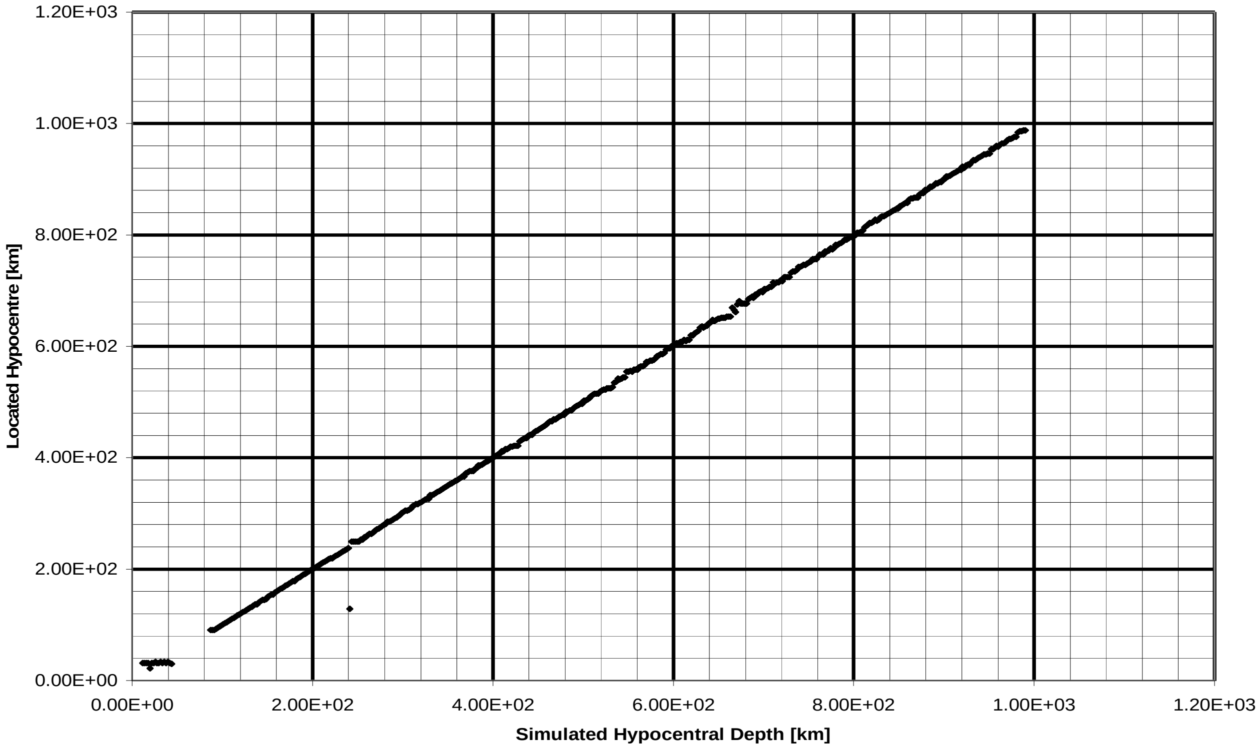

Figure 3. Self-test 03 [Hypocentre (located) vs. Hypocentre (simulated)]

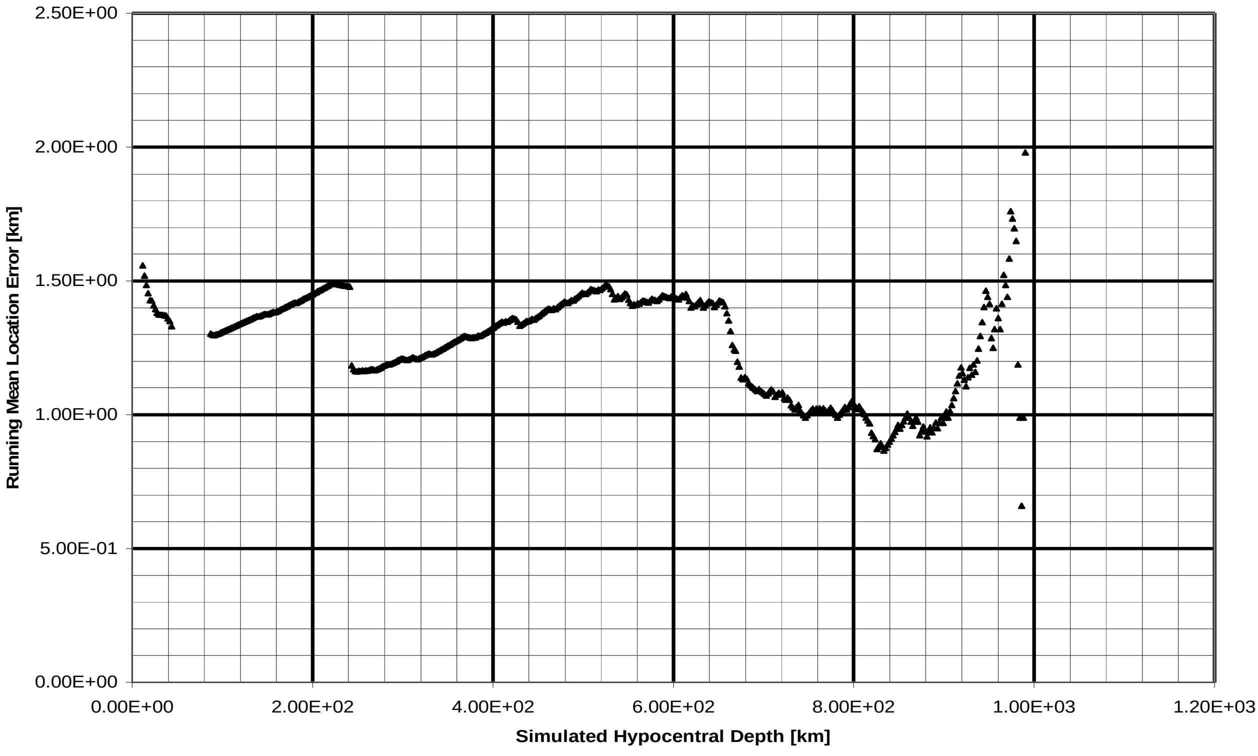

Figure 4. Accumulating Mean Error [Error (km) vs. Hypocentre (simulated)]

ISBN: 978-988-19252-1-3
ISSN: 2078-0958 (Print); ISSN: 2078-0966 (Online)

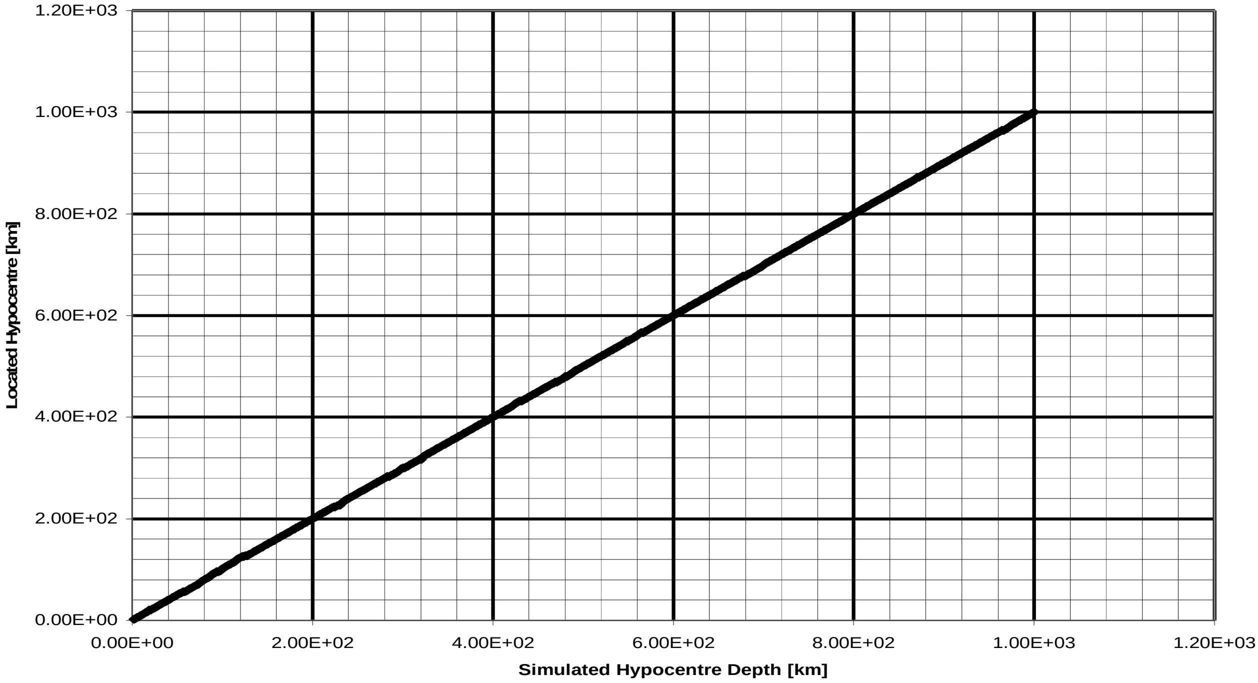

Figure 5. Self-test 18d [Hypocentre (located) vs. Hypocentre (simulated)]

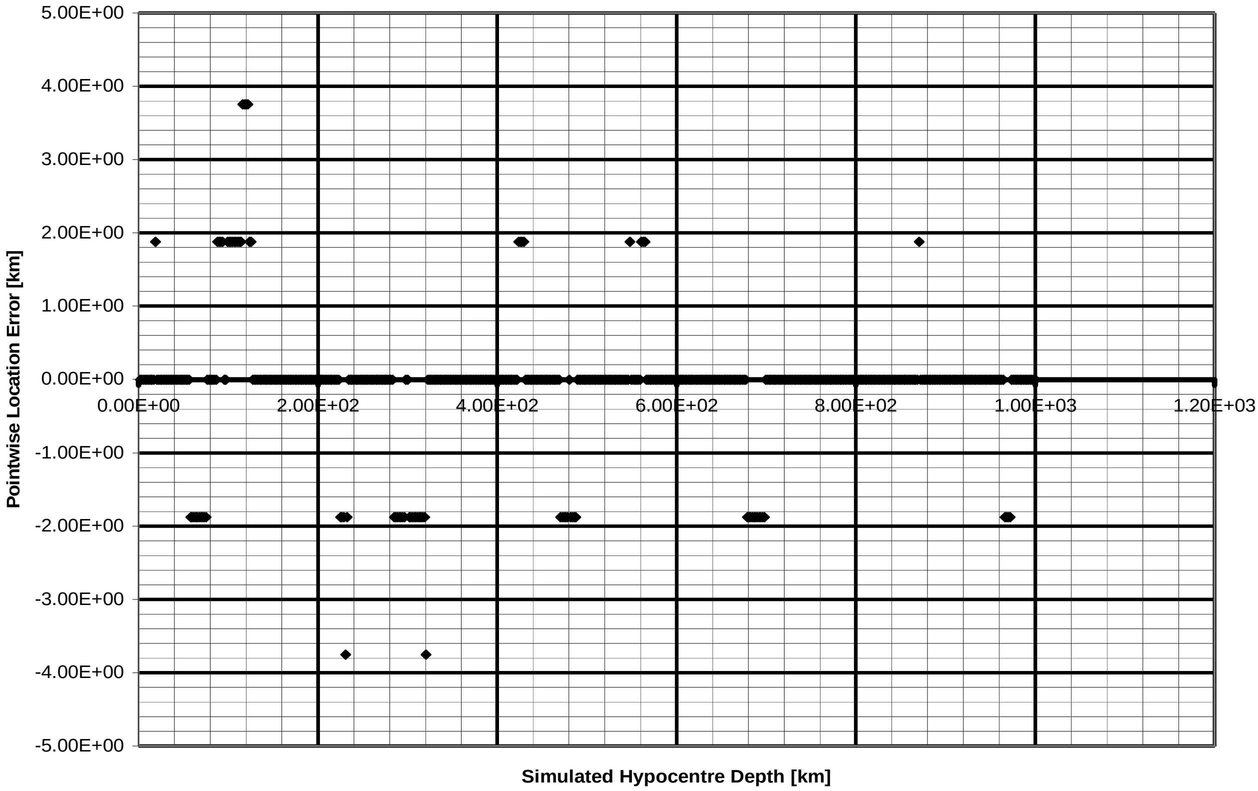

Figure 6. Pointwise Error [Error (km) vs. Hypocentre (simulated)]

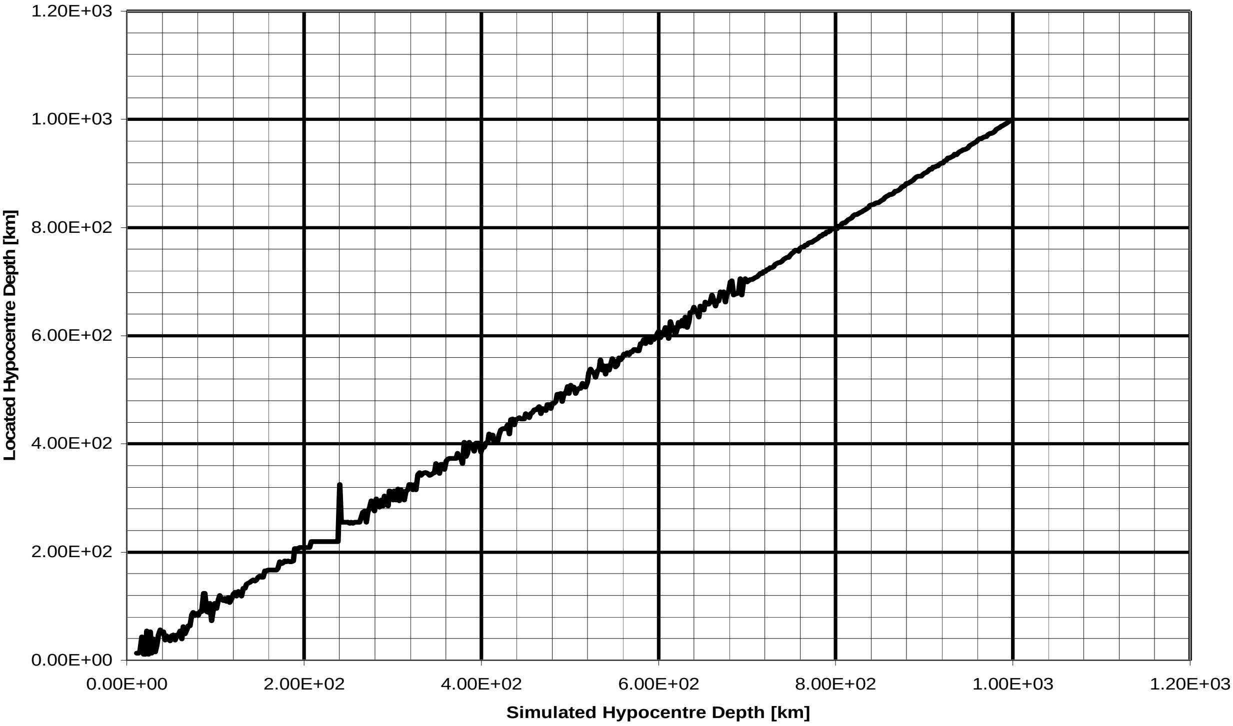

Figure 7. Self-test 09 [Hypocentre (located) vs. Hypocentre (simulated)}

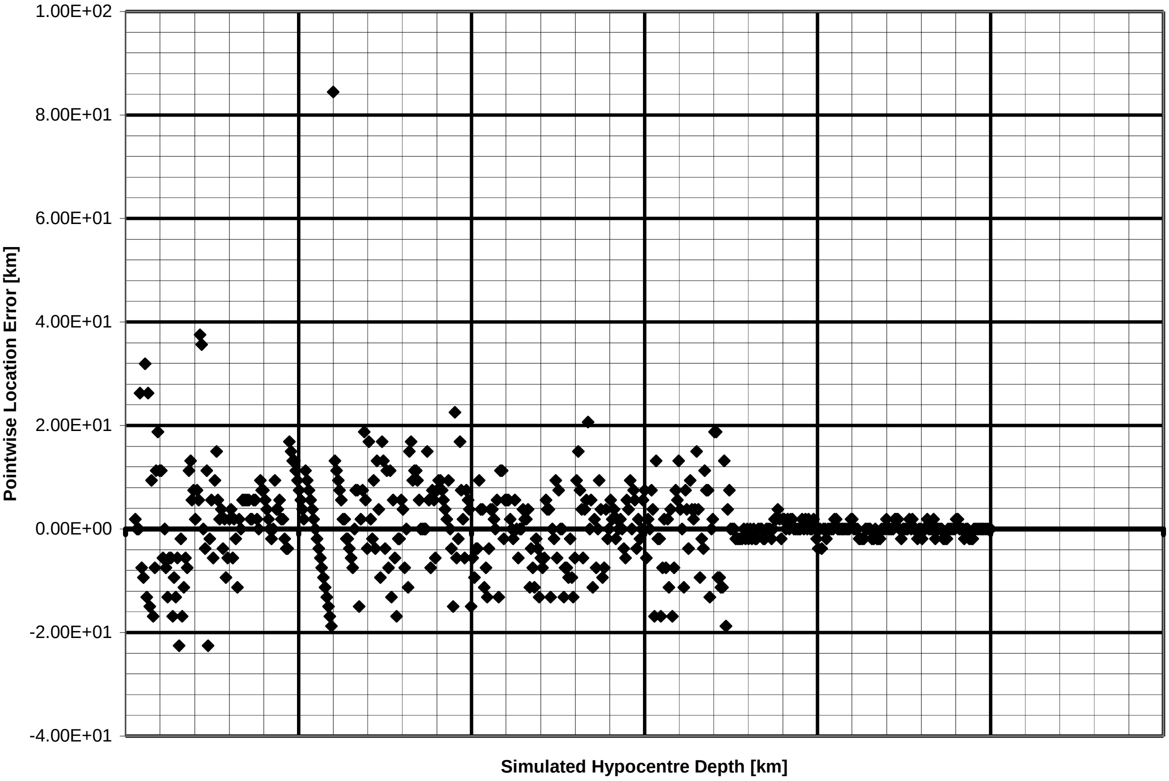

Figure 8. Pointwise Error [Error (km) vs. Hypocentre (simulated)]

ISBN: 978-988-19252-1-3
ISSN: 2078-0958 (Print); ISSN: 2078-0966 (Online)

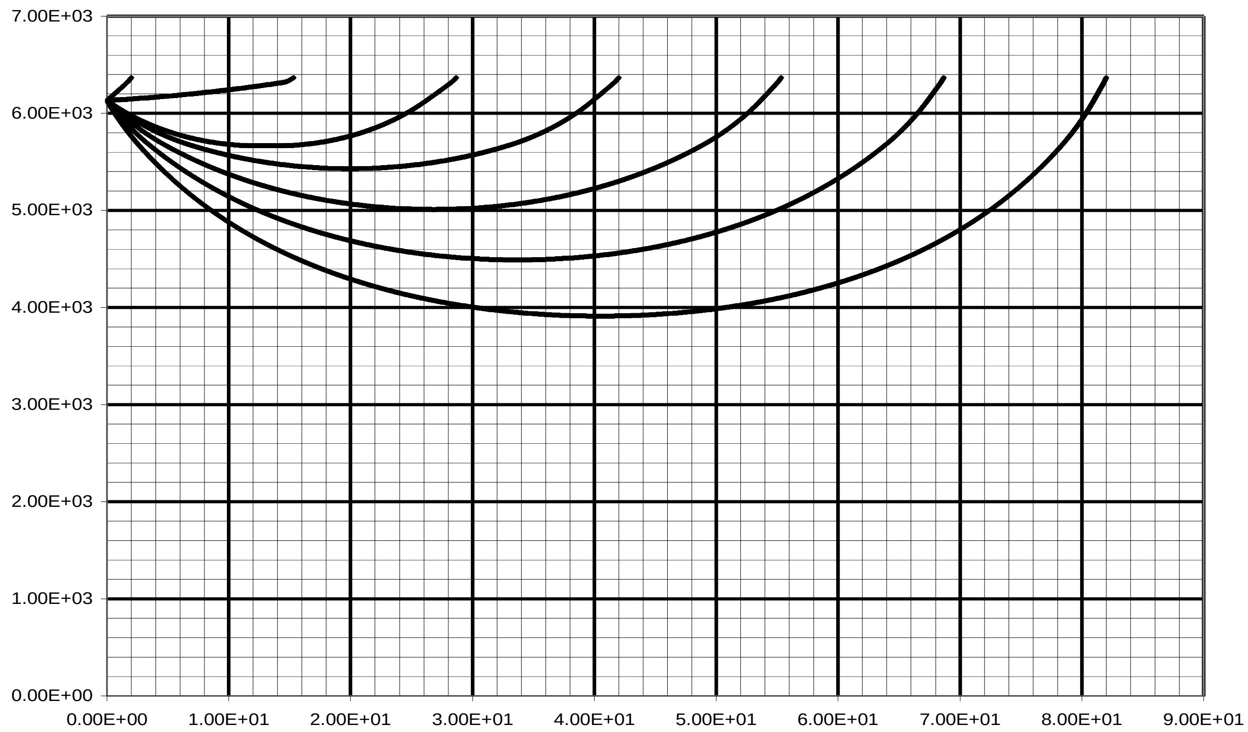

Figure 9. Selected Ray Traces

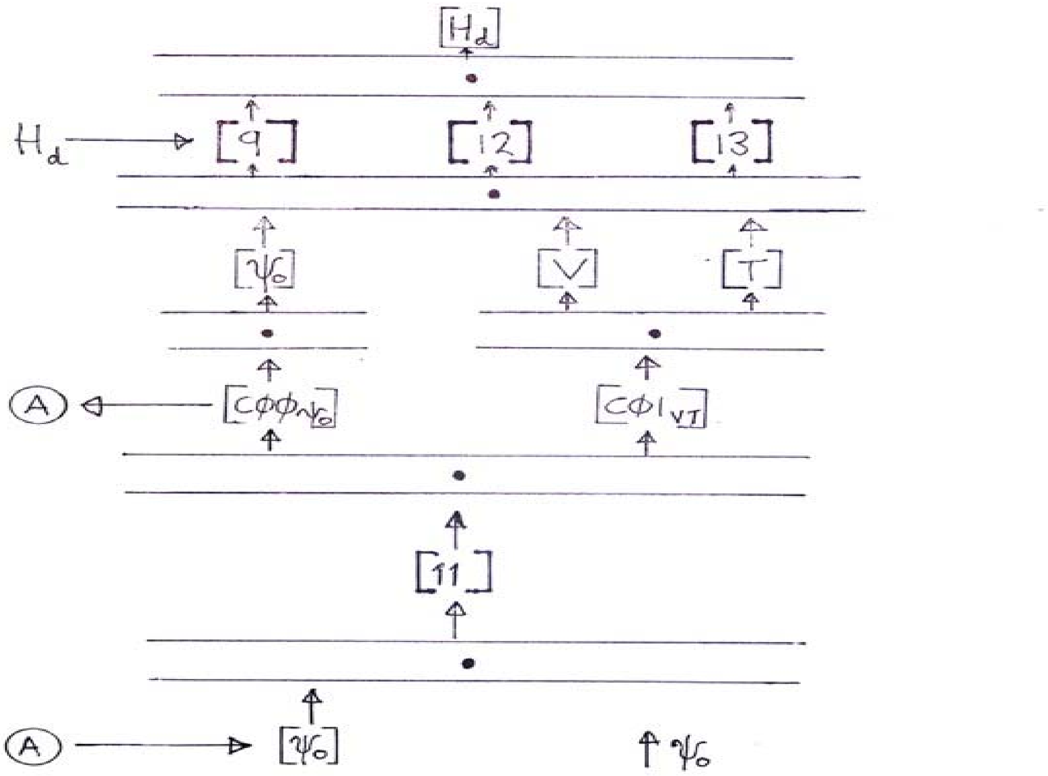

Figure 10. Representative Sub-system Diagram

ISBN: 978-988-19252-1-3
ISSN: 2078-0958 (Print); ISSN: 2078-0966 (Online)